Theoretical Performance Analysis of GNSS Tracking Loops

Conference Paper · May 2023

DOI: 10.1109/PLANS53410.2023.10139980

5 authors, including:

Samy Labsir
Institut Polytechnique des Sciences Avancées

Gael Pages
Institut Supérieur de l'Aéronautique et de l'Espace (ISAE)

Lorenzo Ortega Espluga
Institut Polytechnique des Sciences Avancées

Jordi Vilà-Valls
Institut Supérieur de l'Aéronautique et de l'Espace (ISAE)

Theoretical Performance Analysis of GNSS Tracking Loops

Samy Labsir
IPSA/TéSA
Toulouse, France

Gaël Pages
ISAE-SUPAERO
University of Toulouse
Toulouse, France

Lorenzo Ortega
IPSA/TéSA
Toulouse, France

Jordi Vilà-Valls
ISAE-SUPAERO
University of Toulouse
Toulouse, France

Éric Chaumette
ISAE-SUPAERO
University of Toulouse
Toulouse, France

***Abstract*—This paper aims to characterize the estimation precision at the output of the GNSS receiver tracking stage. We define an original statistical modelling of the GNSS tracking loop, which can then be exploited by an optimal linear Kalman Filter (KF) in order to obtain an analytical expression of the steady-state regime. The latter is designed to encompass dynamic information of the GNSS receiver. Two observation models are of interest: the first one considers the propagation delay and Doppler parameters, and the second one also including the Doppler rate, i.e., the acceleration, which is known to be relevant for high dynamics scenarios and can easily be included into the acquisition step. Within this context, the steady-state asymptotic performance of the tracking stage is obtained by solving an algebraic discrete Riccati equation. In both cases, simulation results are provided to show the validity of the proposed approach and the resulting steady-state performance.**

***Index Terms*—Tracking loop, Kalman filter, maximum likelihood estimator, Riccati equation.**

I. Introduction

There are a huge variety of mass-market and safety-critical applications, within a plethora of engineering fields, where precise and reliable position, velocity and time (PVT) is nowadays of paramount importance, and Global Navigation Satellite Systems (GNSS) [1] is typically the technology of choice to provide positioning information. Therefore, it is fundamental to assess the ultimate achievable performance at each receiver stage, from baseband signal processing to PVT computation. Regarding the first synchronization stage, standard GNSS receiver architectures rely on a scalar (i.e., different satellite signals are processed with independent channels) acquisition and tracking approach. In this case, the former provides a coarse point estimate of the synchronization parameters (identify/acquire visible satellites), and the latter keeps track of their time-varying evolution. These two stages, i.e., acquisition and tracking, can be seen as particular instances of the Maximum Likelihood (ML) solution, where the final goal is to estimate both propagation delay and Doppler shift (or higher order Doppler terms in high dynamics scenarios) for each visible GNSS satellite.

While acquisition and PVT computation are well studied in the literature, the tracking block still needs some further analysis to properly characterize the achievable estimation performance for the time-varying synchronization parameters, which are the input to subsequent code and/or carrier phase-based PVT solvers. In practice, the tracking stage is typically performed using coupled delay/phase/frequency locked loops [2], where the initialization is obtained from the suboptimal ML-based acquisition stage. Considering these loops, the tracking performance (i.e., the achievable delay/Doppler estimation precision under nominal conditions) is not easy to obtain as it depends on several parameters and specific implementations. A possible way to overcome such limitation is to consider a Kalman Filter (KF) based tracking architecture [3], [4], [5], as these locked loops can be seen as suboptimal KF implementations. Using such approach, in its asymptotic regime, the KF estimation error covariance provides the estimation precision on the parameters/states of interest. But standard KF-based tracking schemes are still based on the legacy architecture, that is, they consider a carrier wipe-off, signal correlation, code/phase/frequency discriminators and a linear/extended KF that replaces the standard filter loops.

In this contribution, a fundamentally different approach is proposed to characterize the estimation precision at the output of the tracking stage. The idea is to consider an original statistical modelling of the GNSS tracking loop, which can be exploited by an optimal linear KF in order to obtain an analytical expression of the steady-state regime. As input observations to the filter, two cases are considered: 1) ML-based propagation delay and Doppler measurements, 2) ML-based propagation delay, Doppler and Doppler rate measurements. That is, in the second case the acceleration is also taken into account, a parameter that is relevant for high dynamics scenarios. Indeed, tracking the parameters of the GNSS received signal in a high dynamic context has become a major issue the last years [6], [7], [8], [9], [10], but has not been studied from a statistical point of view.

Considering a large signal-to-noise ratio (SNR) regime, the mean square error (MSE) associated to the ML estimator is known to converge to the corresponding Cramér-Rao bound (CRB), then the uncertainty on the observations taken as input to the KF can be theoretically obtained [11]. In order to obtain the uncertainty for these observations, we consider 1) the closed-form CRB expressions derived for the propagation time and Doppler observation model [12], [13], and 2) the closed-form CRB expression derived for the propagation time,

This work has been partially supported by the DGA/AID projects 2022.65.0082, 2021.65.0070.00.470.75.01, and TéSA.

Doppler and acceleration observation model [14]. Then, a KF is used to recursively estimate the parameters related to propagation time, velocity and acceleration. The advantage of this approach is that it allows to compute theoretically the optimal error covariance matrix. In addition, the steady-state performance of the tracking stage is obtained by solving an algebraic discrete Riccati equation. The latter also allows to characterize the minimum convergence time of the tracking stage. In both cases (i.e., considering or not the acceleration as an input to the filter), results are provided to show the validity of the proposed approach and the resulting steady-state performance.

The article is organized as follows: Section II presents the GNSS received signal model. Section III models the acquisition stage by the ML estimator. Section IV details the proposed tracking loop through the linear KF modelling. Simulation results presented in Section V validate the performance of the proposed method for two particular scenarios. Finally, conclusions are drawn in Section VI

II. Signal model

The complex analytic band-limited signal, with bandwidth B, at the output of the receiver's Hilbert filter, can be written as

$$s_R(t) = \sum_{m=1}^{M} \alpha_m s_m(t-\tau_{A,m}(t)) e^{-j\,2\pi f_c \tau_{A,m}(t)} + n(t), \quad (1)$$

where M is the number of visible satellites, α_m denotes the complex attenuation coefficient and $\tau_{A,m}(t)$ is the propagation delay associated to the m^{th} satellite. $n(t)$ is a zero mean complex white Gaussian noise with unknown variance σ_n^2, f_c is the carrier frequency and $s_m(t-\tau_{A,m}(t))$ is the delayed transmitted signal. In the rest of the paper, and for the sake of notation simplicity, we are only considering one tracking channel, thus allowing to omit the subscript m.

The receiver-satellite distance can be computed as $\rho(t) \triangleq c\,\tau_A(t)$, where c is the speed of light. Note that the distance traveled by the transmitted signal can also be described by

$$\rho(t) = \|\mathbf{p}_S(t-\tau_A(t)) - \mathbf{p}_R(t)\|, \quad (2)$$

with $\mathbf{p}_S(t)$ the satellite position and $\mathbf{p}_R(t)$ the receiver position. Due to the relative radial motion between the satellites and the receiver, the propagation delay is time dependent. A second order distance-velocity-acceleration model yields to

$$\rho(t) \simeq \rho(0) + \|\mathbf{v}_{\text{rel}}\|\, t + \|\mathbf{a}_{\text{rel}}\| \frac{t^2}{2}, \quad (3)$$

or

$$\tau_A(t) = \underbrace{\frac{\rho(0)}{c}}_{=\tau} + \underbrace{\frac{\|\mathbf{v}_{\text{rel}}\|}{c}}_{=b} t + \underbrace{\frac{\|\mathbf{a}_{\text{rel}}\|}{2c}}_{=d} t^2, \quad (4)$$

where b and d relate to the Doppler frequency and the Doppler frequency rate, respectively. For short observation times, and considering a narrowband signal model [12], a good approximation of the Hilbert filter's output yields to

$$s_R(t;\boldsymbol{\eta}) = \tilde{\alpha}\, e^{-j\,2\,\pi\, f_c\,\left(b(t-\tau)+d(t-\tau)^2\right)}\, s(t-\tau) + n(t) \quad (5)$$

with $\boldsymbol{\eta}^\top = [\tau, b, d]$ and $\tilde{\alpha} = \alpha\, e^{-j\,2\,\pi f_c (1+b+d\,\tau)\,\tau}$. Considering the acquisition of N samples at sampling frequency $F_s = B = 1/T_s$, the discrete vector model is

$$\mathbf{s} = \tilde{\alpha}\mathbf{a}(\boldsymbol{\eta}) + \mathbf{n}, \quad (6)$$

with

$$\mathbf{s} = [\ldots,\ s_R(lT_s;\boldsymbol{\eta}),\ \ldots]^\top,$$
$$\mathbf{a}(\boldsymbol{\eta}) = \left[\cdots, e^{-j2\pi f_c\left(b(lT_s-\tau)+d(lT_s-\tau)^2\right)} s(lT_s-\tau), \cdots\right]^\top,$$
$$\mathbf{n} = [\ldots,\ n(lT_s),\ \ldots]^\top,$$

where $l \in (N_1, \cdots, N_2)$ and $\mathbf{n} \sim \mathcal{CN}\left(\mathbf{0}, \sigma_n^2 \mathbf{I}_N\right)$. Note that under a first order approximation, i.e., $d = 0$, we could redefine $\boldsymbol{\eta}^\top = [\tau, b]$, $\tilde{\alpha} = \alpha\, e^{-j\,2\,\pi f_c (1+b)\,\tau}$ and

$$\mathbf{a}(\boldsymbol{\eta}) = \left[\ldots, e^{-j2\pi f_c b(lT_s-\tau)} s(lT_s-\tau), \ldots\right]. \quad (7)$$

III. Acquisition stage

The acquisition stage can be modeled as a Maximum Likelihood Estimator (MLE), and provides the estimated values of the propagation delay, Doppler frequency, and Doppler frequency rate, by computing and maximizing the correlation between the received signal and a noiseless local replica. Considering (6), the vector of estimated parameters $\widehat{\boldsymbol{\eta}}$ is defined as[1] [15]

$$\widehat{\boldsymbol{\eta}}^a = \arg\min_{\boldsymbol{\eta}} \left\{\mathbf{s}^H \boldsymbol{\Pi}^{\perp}_{\mathbf{a}(\boldsymbol{\eta})} \mathbf{s}\right\} = \arg\max_{\boldsymbol{\eta}} \left\{ \frac{\left|\mathbf{a}(\boldsymbol{\eta})^H \mathbf{s}\right|^2}{\mathbf{a}(\boldsymbol{\eta})^H \mathbf{a}(\boldsymbol{\eta})} \right\}. \quad (8)$$

Note that $\widehat{\boldsymbol{\eta}}^a$ provides the initial parameters for the tracking stage, which is defined in the following section. The lowest achievable MSE for this estimator is given by the corresponding CRB. In the case of the signal model defined in (6), the CRB expression was derived in [15], [16],

$$\mathbf{CRB}_{\boldsymbol{\eta}} = \frac{\sigma_n^2}{2\,|\tilde{\alpha}|^2} \mathfrak{Re}\left(\boldsymbol{\Phi}(\boldsymbol{\eta})\right)^{-1} \quad (9)$$

with

$$\boldsymbol{\Phi}(\boldsymbol{\eta}) = \frac{\partial \mathbf{a}(\boldsymbol{\eta})}{\partial \boldsymbol{\eta}^T}^H \boldsymbol{\Pi}^{\perp}_{\mathbf{a}(\boldsymbol{\eta})} \frac{\partial \mathbf{a}(\boldsymbol{\eta})}{\partial \boldsymbol{\eta}^T}. \quad (10)$$

A. Closed-form CRB expression for τ, b and d

The CRBs for the main parameters of interest are:

$$\begin{array}{l} CRB_\tau = \mathbf{CRB}_{\boldsymbol{\eta}}(1,1), \quad CRB_b = \mathbf{CRB}_{\boldsymbol{\eta}}(2,2) \\ CRB_d = \mathbf{CRB}_{\boldsymbol{\eta}}(3,3). \end{array}, \quad (11)$$

A closed-form CRB expression for the bandlimited narrowband signal scenario has been recently computed in [14]:

$$\mathfrak{Re}\left\{\boldsymbol{\Phi}(\boldsymbol{\eta})\right\} = \begin{bmatrix} (\cdot)_{1,1} & (\cdot)_{1,2} & (\cdot)_{1,3} \\ (\cdot)_{1,2} & (\cdot)_{2,2} & (\cdot)_{2,3} \\ (\cdot)_{1,3} & (\cdot)_{2,3} & (\cdot)_{3,3} \end{bmatrix}, \quad (12)$$

[1] Let $S = span\left(\mathbf{A}\right)$ be the linear span of the set of the column vectors of matrix $\mathbf{A}$, $\boldsymbol{\Pi}_{\mathbf{A}} = \mathbf{A}\left(\mathbf{A}^H\mathbf{A}\right)^{-1}\mathbf{A}^H$ is the orthogonal projection over S, and $\boldsymbol{\Pi}^{\perp}_{\mathbf{A}} = \mathbf{I} - \boldsymbol{\Pi}_{\mathbf{A}}$.

with

$$(\cdot)_{1,1} = F_s \begin{pmatrix} W_{3,3} - \frac{|w_3|^2}{w_1} + 4\omega_c^2 d^2 \left(W_{2,2} - \frac{|w_2|^2}{w_1} \right) \\ -4\omega_c d \Im \left\{ W_{3,2} - \frac{w_2^* w_3}{w_1} \right\} \end{pmatrix},$$
$$(\cdot)_{1,2} = F_s \left(2\omega_c^2 d \left(\frac{|w_2|^2}{w_1} - W_{2,2} \right) - \omega_c \Im \left\{ \frac{w_2^* w_3}{w_1} - W_{3,2} \right\} \right),$$
$$(\cdot)_{1,3} = F_s \left(2\omega_c^2 d \left(\frac{w_2 w_4^*}{w_1} - W_{4,2}^* \right) - \omega_c \Im \left\{ \frac{w_4^* w_3}{w_1} - W_{4,3}^* \right\} \right),$$
$$(\cdot)_{2,2} = F_s \left(\omega_c^2 \left(W_{2,2} - \frac{|w_2|^2}{w_1} \right) \right),$$
$$(\cdot)_{2,3} = F_s \left(\omega_c^2 \left(W_{4,2}^* - \frac{w_2 w_4^*}{w_1} \right) \right),$$
$$(\cdot)_{3,3} = F_s \left(\omega_c^2 \left(W_{4,4} - \frac{|w_4|^2}{w_1} \right) \right), \tag{13}$$

where

$$\begin{aligned} & w_1 = \frac{1}{F_s} \mathbf{s}^H \mathbf{s}, \quad w_2 = \frac{1}{F_s^2} \mathbf{s}^H \mathbf{D} \mathbf{s}, \quad w_3 = \mathbf{s}^H \mathbf{\Lambda} \mathbf{s}, \\ & w_4 = W_{2,2} = \frac{1}{F_s^3} \mathbf{s}^H \mathbf{D}^2 \mathbf{s}, \quad w_5 = W_{3,2} = \frac{1}{F_s} \mathbf{s}^H \mathbf{D} \mathbf{\Lambda} \mathbf{s}, \\ & W_{3,3} = F_s \mathbf{s}^H \mathbf{V} \mathbf{s}, \quad W_{4,2} = \frac{1}{F_s^4} \mathbf{s}^H \mathbf{D}^3 \mathbf{s}, \\ & W_{4,3} = W_{5,2} = \frac{1}{F_s^2} \left(\mathbf{s}^H \mathbf{D} \mathbf{\Lambda} \mathbf{D} \mathbf{s} - \mathbf{s}^H \mathbf{D} \mathbf{s} \right), \\ & W_{4,4} = \frac{1}{F_s^5} \mathbf{s}^H \mathbf{D}^4 \mathbf{s}, \end{aligned} \tag{14}$$

with $\mathbf{D}$, $\mathbf{V}$ and $\mathbf{\Lambda}$ defined as

$$\mathbf{D} = \mathrm{diag}\left([N_1, \ N_1 + 1, \ldots, \ N_2 - 1, \ N_2] \right), \tag{15}$$
$$(\mathbf{V})_{l,l'} = \left| \begin{array}{l} l' \neq l : (-1)^{|l-l'|} \frac{2}{(l-l')^2} \\ l' = l : \frac{\pi^2}{3} \end{array} \right., \tag{16}$$
$$(\mathbf{\Lambda})_{n,n'} = \left| \begin{array}{l} l' \neq l : \frac{(-1)^{|l-l'|}}{(l-l')} \\ l' = l : 0 \end{array} \right., \tag{17}$$

The latter is useful and relevant for our study, particularly because we can take advantage of it in the statistical modelling of the tracking stage. Indeed, this allows to properly define the observation model for the linear KF.

B. Closed-form CRB expression for τ and b

For the particular case where the signal model does not consider the acceleration, we have:

$$CRB_\tau = \mathbf{CRB}_{\boldsymbol{\eta}}(1,1), \quad CRB_b = \mathbf{CRB}_{\boldsymbol{\eta}}(2,2). \tag{18}$$

A closed-form CRB expression for the bandlimited narrow-band signal scenario was computed in [12]:

$$\mathfrak{Re}\left\{ \mathbf{\Phi}(\boldsymbol{\eta}) \right\} = \begin{bmatrix} (\cdot)_{1,1} & (\cdot)_{1,2} \\ (\cdot)_{1,2} & (\cdot)_{2,2} \end{bmatrix}, \tag{19}$$

with

$$\begin{aligned} (\cdot)_{1,1} &= F_s \left(W_{3,3} - \frac{|w_3|^2}{w_1} \right), \\ (\cdot)_{1,2} &= F_s \left(-\omega_c \Im \left\{ \frac{w_2^* w_3}{w_1} - W_{3,2} \right\} \right), \\ (\cdot)_{2,2} &= F_s \left(\omega_c^2 \left(W_{2,2} - \frac{|w_2|^2}{w_1} \right) \right). \end{aligned} \tag{20}$$

IV. Kalman Filter Tracking Stage

In order to refine the signal parameters estimates (and track their time-varying evolution), conventional GNSS tracking loops implement a delay-locked loop (DLL) to track the delay variations, and a phase-locked loop (PLL), sometimes assisted by a frequency-locked loop (FLL), to estimate the phase and Doppler frequency variations. The tracking stage is a recursive estimation problem, and the locked loops architecture can be reformulated as a KF. In this study, we propose a linear KF which recursively estimate both state and covariance matrix of the unknown parameters, $\boldsymbol{\eta}_k^\top = [\tau_k, b_k, d_k]$, using the propagation time, Doppler and acceleration observations estimated at the MLE acquisition step.

At the prediction step, a constant acceleration model is considered for the state $\widehat{\boldsymbol{\eta}}_{k|k-1}^t$ evolution (i.e., superscript t for tracking), as it allows to take into account a potential high-dynamic context. At the correction step, the updated state $\widehat{\boldsymbol{\eta}}_{k|k}^t$ is computed using the MLE $\widehat{\boldsymbol{\eta}}_k^a$ measurements (i.e., superscript a for acquisition), computed at each instant k as in (8). We theoretically describe the different steps of the proposed KF model in the sequel.

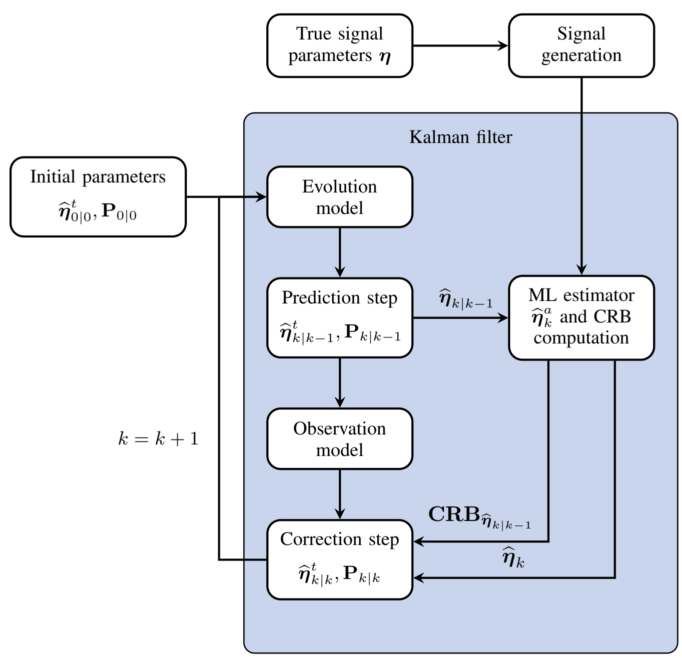

Fig. 1. Principle of the proposed KF-based tracking loop.

A. Evolution model

In order to study the possible influence of a relative acceleration, d_k, when taken into account (or not) within the tracking stage, we consider the following evolution model:

$$\tau_k = \tau_{k-1} + b_{k-1}\,\Delta T + d_{k-1}\,\Delta T^2, \tag{21}$$
$$b_k = b_{k-1} + d_{k-1}\,\Delta T, \tag{22}$$
$$d_k = d_{k-1} + n_d, \quad n_d \sim \mathcal{N}(0, \sigma_d^2), \tag{23}$$

or in compact form,

$$\boldsymbol{\eta}_k = \mathbf{F}\boldsymbol{\eta}_{k-1} + \mathbf{v}_k,\ \mathbf{v}_k \sim \mathcal{N}(\mathbf{0}, \mathbf{Q}), \tag{24}$$

with

$$\mathbf{F} = \begin{bmatrix} 1 & \Delta T & \Delta T^2 \\ 0 & 1 & \Delta T \\ 0 & 0 & 1 \end{bmatrix} \text{ and } \mathbf{Q} = \begin{bmatrix} 0 & 0 & 0 \\ 0 & 0 & 0 \\ 0 & 0 & \sigma_d^2 \end{bmatrix}, \tag{25}$$

where ΔT denotes the time interval between the $(k-1)^{\text{th}}$ and k^{th} discrete time instants, and σ_d^2 represents the dynamic stress noise induced by the receiver motion.

B. Observation model

The observations used within the KF correspond to $\widehat{\boldsymbol{\eta}}_k^a$, computed in (8). Note that since we consider asymptotic conditions, the observations follow a Gaussian distribution whose mean is equal to $\boldsymbol{\eta}_{\boldsymbol{k}}$ and covariance matrix $\mathbf{R}_k$ equal to the $\mathbf{CRB}_{\boldsymbol{\eta}}$ given in Section III. The observation model can be then expressed as:

$$\mathbf{z}_k = \mathbf{H}_k\,\boldsymbol{\eta}_k + \mathbf{u}_k,\ \mathbf{u}_k \sim \mathcal{N}(\mathbf{0}, \mathbf{R}_k),\ \mathbf{R}_k = \mathbf{CRB}_{\widehat{\boldsymbol{\eta}}^t_{k|k-1}}, \tag{26}$$

where 1) $\mathbf{CRB}_{\widehat{\boldsymbol{\eta}}^t_{k|k-1}}$ can be computed from (18) and $\mathbf{H}_k = \mathbf{I}_{2\times 3}$, if the acceleration is not taken into account within the signal model, and 2) $\mathbf{CRB}_{\widehat{\boldsymbol{\eta}}^t_{k|k-1}}$ is equal to (11) and $\mathbf{H}_k = \mathbf{I}_{3\times 3}$, otherwise. Note that if we do not take into account the acceleration, the CRB value does not depend on the parameters but only on the sampling frequency, signal samples and SNR. Thus, for the same receiver conditions it can be assumed constant. Moreover, even if we consider the acceleration but its variation is small, the CRB can also be considered constant (refer to equation (13)). Therefore, in the following we denote $\mathbf{R}_k = \mathbf{R}$.

C. Steady state prediction error covariance

To study the performance of the proposed modelling, it is crucial to know the duration required to obtain a theoretical minimal precision in term of estimation error. In order to characterize the convergence time of the linear KF, it is relevant to use the discrete-time algebraic Riccati equation (DARE) [17], which is extracted from the classical discrete Riccati equation [18], and it provides the predicted covariance obtained for a finite-time horizon. Indeed, if we consider a KF built from the evolution and observation models (24) and (26), then the predicted $\mathbf{P}_{k|k-1}$ covariance and corrected $\mathbf{P}_{k|k}$ covariance follow the classical recursion,

$$\mathbf{P}_{k|k-1} = \mathbf{F}\,\mathbf{P}_{k-1|k-1}\,\mathbf{F}^\top + \mathbf{Q}, \tag{27}$$
$$\mathbf{P}_{k|k} = (\mathbf{I} - \mathbf{K}_k\,\mathbf{H})\mathbf{P}_{k|k-1}, \tag{28}$$
$$\mathbf{K}_k = \mathbf{P}_{k|k-1}\,\mathbf{H}^\top\left(\mathbf{H}\,\mathbf{P}_{k|k-1}\mathbf{H}^\top + \mathbf{R}\right)^{-1}. \tag{29}$$

By substituting (28) and (29) in (27), we obtain the discrete Riccati equation,

$$\begin{aligned}\mathbf{P}_{k|k-1} = &\mathbf{F}\,\mathbf{P}_{k-1|k-2}\,\mathbf{F}^\top - \\ &\mathbf{F}\,\mathbf{P}_{k-1|k-2}\,\mathbf{H}^\top\left(\mathbf{H}\,\mathbf{P}_{k-1|k-2}\,\mathbf{H}^\top + \mathbf{R}\right)^{-1} \\ &\mathbf{H}\,\mathbf{P}_{k-1|k-2}\mathbf{F}^\top + \mathbf{Q}.\end{aligned} \tag{30}$$

In the steady state (convergence), we can set $\mathbf{P} = \mathbf{P}_{k|k-1} = \mathbf{P}_{k-1|k-2}$, $\forall\, k$, which leads to the following DARE,

$$\mathbf{P} = \mathbf{F}\,\mathbf{P}\,\mathbf{F}^\top - \mathbf{F}\,\mathbf{P}\,\mathbf{H}^\top\left(\mathbf{H}\,\mathbf{P}\,\mathbf{H}^\top + \mathbf{R}\right)^{-1}\mathbf{H}\,\mathbf{P}\mathbf{F}^\top + \mathbf{Q}. \tag{31}$$

V. Simulation results

The objective of this section is to study the asymptotic performance of the proposed tracking loop architecture taking into account the acceleration in the evolution model. Consequently, we focus on the characterization of the predicted and corrected covariance estimation matrices of the linear KF. Two scenarios are considered:

- In the first scenario (S1) the acceleration (as a measurement) is not taken into account in the signal model (6). Note that this is a misspecified signal model [19].
- In the second scenario (S2) the acceleration is preserved in the signal model [14].

In each scenario, we are interested in quantifying the delay and Doppler frequency estimation precision for high-dynamic targets, i.e., when σ_d is large. On the other hand, we also study the methods' convergence with the DARE solution.

A. Experiments

At the receiver, we consider a GPS L1 C/A signal sampled at $F_s = 2$ MHz, and with an integration time equal to 4 ms. We also consider $\Delta T = 4$ ms. To evaluate the theoretical filtering performance, we are interested on the behaviour of the prediction error covariance matrix as a function of $c\,\sigma_d$ and the number of iterations considered to compute the DARE solution. Then, we need to set the SNR at the output of the matched filter [12],

$$SNR_{OUT} = \frac{|\tilde{\alpha}|\boldsymbol{s}^H\boldsymbol{s}}{\sigma_n^2}. \tag{32}$$

1) Study of the impact of σ_d: first, we define the covariance ratio matrix, computed at each instant k for each state vector component $i \in \{1, 2, 3\}$,

$$(r_k)_i = \frac{[\mathbf{P}_{k|k}]_{i,i}}{[\mathbf{R_k}]_{i,i}}, \tag{33}$$

where $[\mathbf{P}_{k|k}]_{i,i}$, or $[\mathbf{P}_{k|k}]_i$ for sake of simplicity, is the estimated variance for component i. Then, we study the evolution

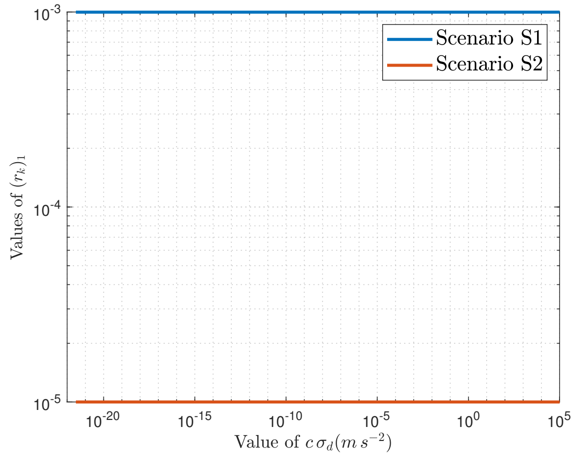

Fig. 2. Evolution of r_k for parameter τ_k versus $c \cdot \sigma_d$

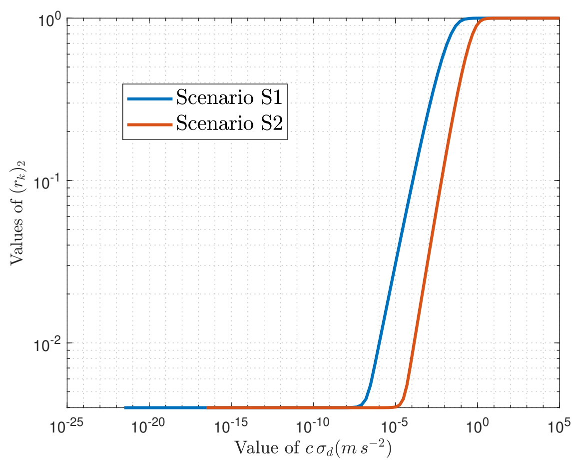

Fig. 3. Evolution of r_k for parameters b_k versus $c \cdot \sigma_d$.

of such ratio for both parameters τ_k and b_k. We consider 1000 iterations.

Fig. 2 shows the covariance matrix ratio for the parameter τ_k, i.e., $(r_k)_1$, for both scenarios S1 and S2, considering a SNR_{OUT} = 20dB. Note that negligible variations of the covariance ratio are observed. Although the value of the covariance ratio is lower in S2 (around 1 order of magnitude), we can fairly conclude that σ_d has no direct impact on the propagation delay estimation. However, this is different for the parameter b_k, as it can be seen in Fig. 3. For S1, at low values of $c \cdot \sigma_d$ (between 10^{-20}m.s^{-2} and 10^{-1}m.s^{-2}) the covariance matrix ratio is near zero, which means a good estimation of the b_k parameter. Note that this is an expected result since low values of $c \cdot \sigma_d$ involve low dynamics, i.e., no impact of the Doppler rate. When $c \cdot \sigma_d$ increases, the $(r_k)_2$ raises, loosing precision as the dynamics increase, reaching a flat region (around 10^0m.s^{-2}) where the KF can not improve the estimation performance. For S2, even if the same behaviour is observed, the transition region starts at a larger $c \cdot \sigma_d$ value,

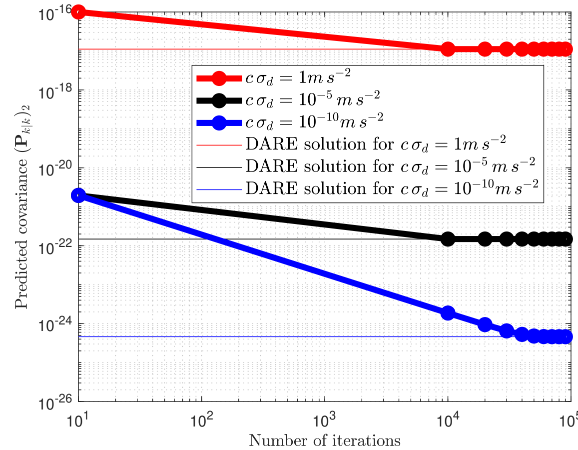

Fig. 4. Evolution of $[\mathbf{P}_{k|k-1}]_2$ to the DARE solution as a function of the number of iterations. Scenario S1.

showing the interest of taking into account the acceleration as a measurement under certain conditions (i.e., high-dynamic).

2) Analysis of the DARE solution: Figs. 4 and 5 show the evolution of both covariance matrix estimation $[\mathbf{P}_{k|k-1}]_2$ and the DARE solution for the parameter b_k, considering different values of $c \cdot \sigma_d$. For this particular scenario, we consider 10000 iterations and SNR_{OUT} = 20dB. We observe that in S1, the speed of convergence of the variance (to the Riccati solution (31)) is faster when the value of σ_d increases. On the other hand, even if the same behaviour is observed in S2, the convergence is globally faster due to the fact that d_k is considered within the observation model, i.e., the DARE solution converges faster (10^4 iterations in S1 against 10^3 in S2).

Figs. 6 and 7 show the evolution of the DARE solution as a function of $c \cdot \sigma_d$, for different values of SNR_{OUT}, in order to quantify its impact on the estimation performance. Again, we consider 10000 iterations. In S1, we note that the predicted covariance matrix element $[\mathbf{P}_{k|k-1}]_2$ converges faster to the DARE solution with higher SNR_{OUT}. Moreover, we see that the DARE solution converges to the same value when σ_d is large whatever the SNR_{OUT}. In S2, since the acceleration is taken into account in the observation model, we observe faster convergence to the DARE solution as well as an improvement of the precision performance.

VI. Conclusions

In this article, we proposed to model the GNSS tracking loop through a linear Kalman filter, considering the acceleration within the observation model. The acceleration information is extracted from the maximum likelihood estimator, which is known to be asymptotically efficient. Then, thanks to this new architecture and considering the asymptotic SNR regime, we provided closed-form expressions of the theoretical performance of the tracking loop, being this the discrete-time algebraic Riccati equation. Results were provided to check the validity of such closed-form expression. Moreover,

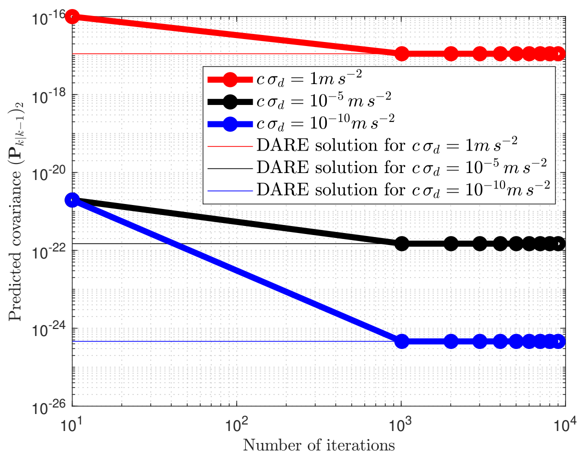

Fig. 5. Evolution of $[\mathbf{P}_{k|k-1}]_2$ to the DARE solution as a function of the number of iterations. Scenario S2.

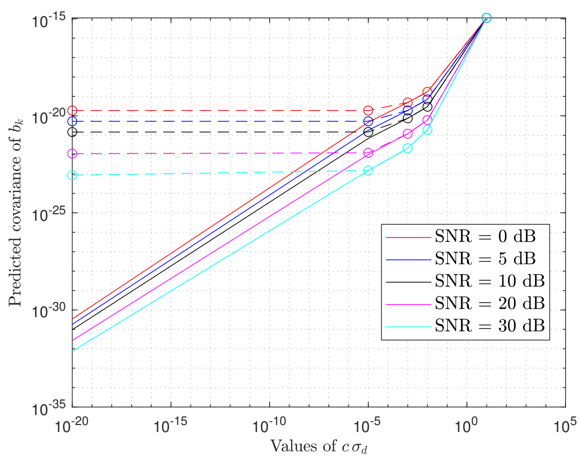

Fig. 6. Evolution of $[\mathbf{P}_{k|k-1}]_2$ (thick line) to the DARE solution (dot line) as a function of $c \cdot \sigma_d$ for different values of SNR_{OUT}. Scenario S1.

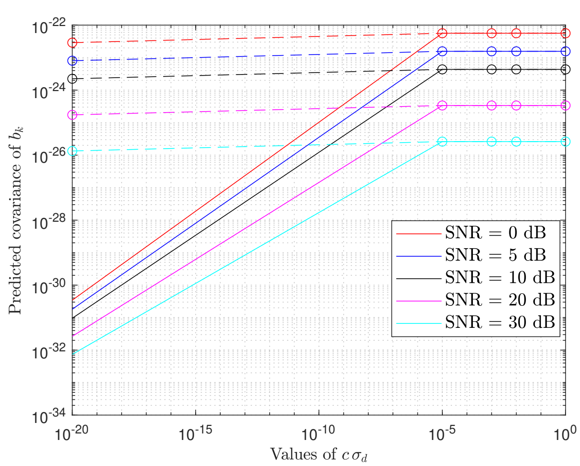

Fig. 7. Evolution of $[\mathbf{P}_{k|k-1}]_2$ (thick line) to the DARE solution (dot lines) as a function of $c \cdot \sigma_d$ for different values of SNR_{OUT}. Scenario S2.

the proposed architecture was tested and validated through numerical simulations, to study the impact of high-dynamics on the precision and convergence of the linear Kalman filter theoretical performance.

References

[1] P. J. G. Teunissen and O. Montenbruck, Eds., *Handbook of Global Navigation Satellite Systems*, Springer, Switzerland, 2017.

[2] E. Kaplan and C. J. Hegarty, *Understanding GPS: Principles and Applications*, Artech House, Inc., USA, 2nd edition, 2005.

[3] J.-H. Won, T. Pany, and B. Eissfeller, "Characteristics of kalman filters for gnss signal tracking loop," *IEEE Transactions on Aerospace Electronic Systems*, vol. 48, pp. 3671–3681, 10 2012.

[4] Y. Yang, J. Zhou, and O. Loffeld, "GPS receiver tracking loop design based on a Kalman filtering Approach," in *Proceedings ELMAR-2012*, 01 2012, pp. 121–124.

[5] M. Susi and D. Borio, "Kalman filtering with noncoherent integrations for Galileo E6-B tracking," *NAVIGATION: Journal of the Institute of Navigation*, vol. 67, no. 3, pp. 601–617, 2020.

[6] P. Roncagliolo, C. E. De Blasis, and C.H. Muravchik, "GPS Digital Tracking Loops Design for High Dynamic Launching Vehicles," in *2006 IEEE Ninth International Symposium on Spread Spectrum Techniques and Applications*, 2006, pp. 41–45.

[7] P. Roncagliolo and J. Garcia, "High dynamics and false lock resistant GNSS carrier tracking loops," in *Proceedings of the 20th International Technical Meeting of the Satellite Division of The Institute of Navigation (ION GNSS 2007)*, 09 2007, vol. 2, pp. 2364–2375.

[8] Qiliang Chen, Xiongjun Wu, Jiahong Liang, and Chan Zeng, "An ekf based tracking loop filter algorithm in gnss receiver for ultra high dynamic environment: The experiment results," in *IECON 2018 - 44th Annual Conference of the IEEE Industrial Electronics Society*, 2018, pp. 2802–2808.

[9] Qinghua Zeng, Wenqi Qiu, Jianye Liu, Rui Xu, Jinheng Shi, and Yongrong Sun, "A high dynamics algorithm based on steepest ascent method for GNSS receiver," *Chinese Journal of Aeronautics*, vol. 34, no. 12, pp. 177–186, 2021.

[10] R. Mu and T. Long, "Design and implementation of vector tracking loop for high-dynamic gnss receiver," *Sensors*, vol. 21, pp. 5629, 08 2021.

[11] H. L. Van Trees and K. L. Bell, Eds., *Detection, Estimation and Modulation Theory - Part 1*, Wiley/IEEE Press, New-York, NY, USA, 2013.

[12] D. Medina, L. Ortega, J. Vilà-Valls, P. Closas, F. Vincent, and E. Chaumette, "Compact CRB for Delay, Doppler and Phase Estimation - Application to GNSS SPP & RTK Performance Characterization," *IET Radar, Sonar & Navigation*, vol. 14, no. 10, pp. 1537–1549, Sep. 2020.

[13] Priyanka Das, Lorenzo Ortega, Jordi Vilà-Valls, François Vincent, Eric Chaumette, and Loïc Davain, "Performance Limits of GNSS Code-Based Precise Positioning: GPS, Galileo & Meta-Signals," *Sensors*, vol. 20, no. 8, pp. 2196, 2020.

[14] H. McPhee, L. Ortega, J. Vilà-Valls, and E. Chaumette, "Accounting for acceleration ; signal parameters estimation performance limits in high dynamics applications," *IEEE Transactions on Aerospace and Electronic Systems*, pp. 1–13, 2022.

[15] Ottersten, B. and Viberg, M. and Stoica, P. and Nehorai, A., *Exact and Large Sample Maximum Likelihood Techniques for Parameter Estimation and Detection in Array Processing*, pp. 99–151, Springer Berlin Heidelberg, Berlin, Heidelberg, 1993.

[16] H. L. Van Trees, Ed., *Optimum Array Processing*, Wiley-Interscience, New-York, NY, USA, 2002.

[17] V. Kučera, *Algebraic Riccati Equation: Hermitian and Definite Solutions*, pp. 53–88, Springer Berlin Heidelberg, Berlin, Heidelberg, 1991.

[18] A. A. Stoorvogel and A. Saberi, "The discrete algebraic riccati equation and linear matrix inequality," in *Proceedings of 1994 33rd IEEE Conference on Decision and Control*, 1994, vol. 2, pp. 1511–1516 vol.2.

[19] H. McPhee, L. Ortega, J. Vilà-Valls, and E. Chaumette, "On the accuracy limits of misspecified delay-doppler estimation," *Signal Processing*, vol. 205, pp. 108872, 2023.